Biofilm 7 (2024) 100198

Contents lists available at ScienceDirect

Biofilm

journal homepage: www.sciencedirect.com/journal/biofilm

Farnesol repurposing for prevention and treatment of *Acinetobacter baumannii* biofilms

Li Tan, Rong Ma, Adam J. Katz, Nicole Levi *

Department of Plastic and Reconstructive Surgery, Wake Forest University School of Medicine, Winston-Salem, North Carolina, USA

ARTICLE INFO

Keywords:
Farnesol
Acinetobacter baumannii
Multidrug-resistant
Biofilms

ABSTRACT

Acinetobacter baumannii has emerged as a multidrug-resistant (MDR) superbug by causing severe infections, with high mortality rates. The ability of *A. baumannii* to form biofilms significantly contributes to its persistence in diverse environmental and hospital settings. Here we report that farnesol, an FDA-approved commercial cosmetic and flavoring agent, demonstrates efficacy for both inhibition of biofilm formation, and disruption of established *A. baumannii* biofilms. Moreover, no resistance to farnesol was observed even after prolonged culture in the presence of sub-inhibitory farnesol doses. Farnesol combats *A. baumannii* biofilms by direct killing, while also facilitating biofilm detachment. Furthermore, farnesol was safe, and effective, for both prevention and treatment of *A. baumannii* biofilms in an *ex vivo* burned human skin model. Since current treatment options for *A. baumannii* biofilm infections were mainly counted on the combination therapy of last-resort antibiotics, and clearly non-sustainable due to robust MDR phenotype of *A. baumannii*, we propose that farnesol alone can be repurposed as a highly effective agent for both preventing and treating life-threating biofilm-associated infections of *A. baumannii* due to its proven safety, convenient topical delivery, and excellent efficiency, plus its superiority of evading resistance development.

1. Introduction

Since persistent use of antibiotics has driven the emergence of multidrug resistant (MDR) bacteria, which renders the originally effective drugs ineffective [1], the global dissemination of antibiotic resistance is one of the greatest challenges in modern medicine. Gram-negative *Acinetobacter baumannii* is one of the most troublesome MDR bacterial pathogens, causing 5–10 % of nosocomial infections worldwide [2]. It has been reported to cause a variety of hospital and community-acquired infections, including pneumonia, bloodstream, skin and soft tissue infections, urinary tract infections, and meningitis [3,4]; moreover, the infections are associated with high mortality rates approaching 70 % [5]. What's worse, *A. baumannii*'s emerging resistance to last-resort antibiotics, (e.g., colistin, tigecycline, and carbapenems) instigates fear of a lack of future treatment options [6–8]. Thus, the World Health Organization has assigned *A. baumannii* as a critical (Priority 1) pathogen posing a great threat to human health, for which new antibiotics/treatments are desperately needed [9].

A. baumannii biofilms consist of a structured community of bacteria encased in a self-produced polymeric matrix which is adherent to biotic and abiotic surfaces [10]. The capacity of *A. baumannii* to form biofilms on medical devices such as catheters and ventilators contributes to its chronic and persistent infections, especially in hospital settings. Since biofilm-embedded cells have limited metabolic activity and are protected by the biofilm matrix, they can be up to 1000-fold more resistant to antibiotics than their planktonic counterparts [11]. As a result, disrupting established *A. baumannii* biofilms is extremely challenging due to its MDR phenotype. Currently there are a lack of agents capable of either prevention or treatment of *A. baumannii* biofilm-associated infections.

Farnesol, a colorless sesquiterpenoid alcohol with a sweet odor, is commonly found in essential oils and plant-derived foods [12]. It is a GRAS (generally recognized as safe) compound, and has been approved by the Food and Drug Administration (FDA) as a flavoring agent widely applied in the food, cosmetic and perfume industries [13–15]. Since farnesol was first found to inhibit filamentation and biofilm formation of the fungus *Candida albicans* in 2002 [16], it has shown versatile functions as an antimicrobial, antitumoral, cardioprotective, hepaprotective, and neuroprotective agent [17–21]. Farnesol has been generally acknowledged to be effective at inhibiting growth of Gram-positive

* Corresponding author. 27157, USA.
E-mail address: nlevi@wakehealth.edu (N. Levi).

https://doi.org/10.1016/j.bioflm.2024.100198
Received 25 January 2024; Received in revised form 17 April 2024; Accepted 19 April 2024
Available online 20 April 2024

bacteria, but its efficacy against Gram-negative bacteria, especially *A. baumannii*, depend upon the strains [22–24]. Kostoulias et al. show differences in farnesol effects on planktonic *A. baumannii* growth dependent upon the strains, and highlight both biofilm decreases and increase by farnesol treatment, again dependent upon the strains. Most significantly, they showed that farnesol was ineffective against MDR strains [24]. Moreover, farnesol has only minor effects on disrupting established biofilms for both Gram-positive and negative bacteria [13,22,25–27]. Given its benefits, farnesol has been suggested as a potential adjuvant for conventional antibiotics due to its synergistic effects [23,28–30]. However, farnesol alone was not considered to be effective enough as an antimicrobial agent by itself [23].

In the current work we selected ethanol as an optimal vehicle for farnesol to reach the highest stock concentration of 30 mg/ml, and demonstrate that concentrated (up to 15 mg/ml) farnesol in ethanol is highly effective for both preventing biofilm formation, and also disrupting established biofilms of *A. baumannii* both *in vitro* and *ex vivo*. Previous publications have used methanol [24], Tween 80 [31], or dimethyl sulfoxide [32] as a carrier solvent, but much lower concentrations were achievable compared to our formulation. Thus, the high potency of farnesol in ethanol is proposed to be an effective agent to both prevent and treat biofilm–associated infections of *A. baumannii*.

2. Materials and methods

2.1. Bacterial strains and culture

Bacterial strains used in this study were *A. baumannii* type strain ATCC 19606, first isolated from a patient urine sample over 70 years ago [33], BAA-1605, a MDR clinic strain isolated from the sputum of a soldier returning from Afghanistan in 2006, and ATCC 17978, which was isolated from a fatal case of meningitis in a 4-month-old infant [34]. Nutrient broth (NB, Becton Dickinson) broth/agar was used to culture *A. baumannii*. Before each experiment, inoculum from a frozen stock was grown overnight on an NB plate at 37 °C. One isolated colony was then used to inoculate a fresh culture. Bacteria were cultured overnight at 37 °C, with shaking at 160 rpm, and then centrifuged at 2500×*g* for 10 min. The pellet was resuspended in fresh broth, followed by the measurement of optical density at 600 nm (OD600). The concentration of colony-forming units (CFU)/ml was then calculated based on a conversion formula correlating OD600 to CFUs (Fig. S1, see below for details). The bacteria were then diluted to the desired concentrations (1×10^6 CFU/ml for biofilm formation, or 1×10^8 CFU/ml for established biofilms, unless otherwise stated). For CFU counting, samples were serially diluted, and drop-plated on NB plate [35].

2.2. Conversion between OD600 and CFU/ml

To obtain the formula for conversion between OD600 and CFU/ml, a bacterial pellet was re-suspended in NB and its OD600 was measured. The bacterial culture was then serially diluted to obtain OD600 readings of ~0.1, 0.2, 0.4, 0.8 in NB. The CFU/ml of viable bacteria for each OD600 value was determined by serial dilutions and drop plating. The linear relationship for conversion between OD600 and CFU/ml for each strain, and their individual coefficient of determination (R^2) values were analyzed using GraphPad Prism 9 (version 9.2.0).

2.3. Inhibition of biofilm formation

Biofilms were started from the overnight bacterial cultures as described above. Polystyrene plates (96 well) were coated with 100 μl of 20 % filtered, apheresis-derived pooled human plasma (Innovative Research) in 50 mM sodium bicarbonate (Sigma) for 24 h at 4 °C. In the coated wells, bacteria (1×10^6 CFU/ml) were cultured in 100 μl of NB containing farnesol (Cayman Chemical, prepared as a 30 mg/ml of stock in ethanol, stored at −20 °C, and diluted to various final concentrations with NB at the time of inoculation). As a vehicle control, bacteria were exposed to the NB containing the same amount of ethanol, but without farnesol. After 24-h incubation at 37 °C in a humidified container, planktonic cells were removed, biofilms were washed with 100 μl of phosphate buffered saline (PBS), adherent bacteria were dislodged in 100 μl of PBS by vigorous (≥10 times) pipetting, and the CFU/ml of viable bacteria was determined by serial dilutions and drop plating. The lower limit of detection was 50 CFU/ml. To visualize the data on a logarithmic scale, a value of 50 CFU/ml was assigned when no growth occurred.

2.4. Treatment of established biofilms

Biofilms were established by culturing 250 μl of NB containing innocula (1×10^8 CFU/ml) in a plasma-coated 96-well plate at 37 °C. After a 24-h incubation in a humidified container, planktonic cells were removed, and the established biofilms were washed with 250 μl of PBS, and then exposed to 100 μl of various final concentrations of farnesol in NB. After an additional 24-h incubation in a humidified container, supernatant was removed, adherent biofilms were washed with 100 μl of PBS, dislodged in 100 μl of PBS by vigorous (≥10 times) pipetting, and the CFU/ml of viable bacteria was determined by serial dilutions and drop plating. Biofilms were exposed to the same amount of ethanol in NB as a vehicle control.

2.5. Live/dead viability assay

The effect of farnesol on biofilm formation and established biofilms of *A. baumannii* was visualized by FilmTracer™ (Invitrogen) Live/Dead biofilm viability assay. Biofilms were established by culturing 500 μl of NB containing innocula (1×10^6 CFU/ml plus farnesol for biofilm formation; 1×10^8 CFU/ml for established biofilms) in chambers of a 4-well Lab-Tek™ chambered coverglass (Nunc) pre-coated with 500 μl of human plasma as described above. After 24-h incubation in a humidified container, planktonic cells were removed, and biofilms were washed with 500 μl of sterile water (for biofilm formation) or PBS (for established biofilms). Established biofilms were then exposed to 500 μl of farnesol in NB for an additional 24 h in a humidified container, then supernatant was removed, and adherent biofilms were washed with 500 μl of sterile water. The obtained biofilms were stained 20–30 min at room temperature with 250 μl of a mixture containing 10 μM of SYTO® 9 green fluorescent nucleic acid stain and 60 μM of propidium iodide (PI) red-fluorescent nucleic acid stain, while protected from light. The biofilms were then washed with 250 μl of sterile water, covered with 300 μl of sterile water, and observed using a Keyence® BZ-X800/BZ-X810 All-in-One fluorescence microscope. The obtained biofilm images were analyzed using Photoshop® to quantify fluorescence intensity and Comstat2 (www.comstat.dk) to evaluate three-dimensional biofilm structure, and quantify biomass and average thickness of the biofilms [36,37].

For some experiments, following farnesol treatment, the supernatant containing detached cells (400 μl) were transferred into a sterile tube, centrifuged at 17,000×*g* for 5 min, then the supernatant was removed, and the pellet was washed with 1 ml of sterile water. The washed pellet was then re-suspended and stained with the 250 μl of the SYTO® 9-PI mixtures described above, and centrifuged to remove unbound fluorescent dyes, washed with 1 ml of sterile water, re-suspended in 300 μl of sterilized water, and transferred into another plasma pre-coated chambered coverglass. The stained cells were allowed to settle at room temperature for 30 min while protected from light, and then were imaged using the Keyence® microscope.

2.6. Resistance development

Development of resistance to farnesol was evaluated as previously described [38]. For comparison, development of resistance to the

clinically relevant antibiotic rifampicin (Bedford Laboratories) was tested as a positive control. Briefly, 5 μL of *A. baumannii* ATCC 19606 inoculum (1×10^8 CFU/ml) was combined with 95 μl of NB containing farnesol (with final concentrations ranging from 0.016 to 2 mg/ml), or rifampicin (with final concentrations ranging from 0.125 to 16 μg/ml for first passage). Plates were sealed with two layers of parafilm and incubated overnight at 37 °C and shaking at 160 rpm. The MIC, the lowest concentration of farnesol or rifampicin that caused lack of visible bacterial growth, was visually determined. Thereafter, the obtained 0.5-fold MIC suspension was diluted ten-fold with fresh NB, and 5 μl of the diluent was then added to 95 μl of fresh NB containing serial dilutions (with updated concentrations if needed) of farnesol or rifampicin, and these mixtures were incubated as described above for the next passage. The ranges of farnesol or rifampicin concentrations were gradually increased, based on the daily-updated MIC results. This was repeated for 20 continuous passages.

2.7. Propidium iodide (PI) influx assay

Bacterial biofilms were established in plasma-coated 96-well plates described as above. Washed biofilms were then exposed to 20 μM of PI (Invitrogen) at room temperature for 10 min, protected from light. Farnesol was then added into each well to reach various final concentrations in a total volume of 150 μl, and incubated at room temperature for 30 min, protected from light. Unbound PI was then gently removed from each well and the biofilms were washed with 150 μl of sterile water, followed by the addition of 100 μl of sterile water into each well. PI fluorescence was then measured every 30 s for 5 min using a TECAN Infinite M200 microplate reader. As a vehicle control, biofilms were exposed to the same amount of ethanol without farnesol.

2.8. Infection and treatment of ex vivo human skin

Human skin was obtained from healthy donors undergoing abdominoplasty in the Department of Plastic and Reconstructive Surgery at Wake Forest University School of Medicine, under an Institutional Review Board (IRB)-approved protocol. The human samples were de-identified, and classified as human waste, hence no informed consent needed. None of the authors were involved in the tissue procurement. Skin samples were processed within an hour after surgery, and excess subcutaneous fat was removed. Three centimeter portions of skin were cut and the epidermis was sprayed with 70 % ethanol for 5 min, then soaked with sterile PBS (~50 ml/sample) for 10 min (total 4 cycles of soaking to remove any potential blood, bacteria, or chemical residues). Burns were induced on the skin surface using a 3-cm diameter brass cylinder heated to 100 °C in 200 mM of polyethylene glycol solution for 10 s. The weight of the cylinder provided a consistent pressure (345 g) that was applied to the human skin during burn creation to induce a second-degree burn injury. The skin was then placed (epidermal side up) into one well of a 6-well plate containing 1 ml of Dulbecco's modified Eagle's medium (DMEM, Gibco) complemented with 2 mM of glutamine and 10 % heat-inactivated fetal bovine serum (HI-FBS, Gibco). Only the lower dermis of the skin was immersed in the medium. Half of the soaked skin samples were retained as intact/unburned controls.

For biofilm experiments with skin, 50 μl of bacterial inoculum (1×10^5 CFU/ml containing farnesol for biofilm formation, or 1×10^7 CFU/ml for established biofilms) was evenly distributed onto the intact or burned skin. The plates were incubated at 37 °C and 5 % CO_2 for 24 h in a humid chamber. For treatment of 24-h-old established biofilms, 100 μl of NB containing farnesol was evenly distributed onto the established biofilms on skin surfaces and then incubated at 37 °C and 5 % CO_2 for an additional 24 h. As a control, samples were exposed to the vehicle (ethanol) without farnesol.

To assess the viable bacterial count, three 5-mm punch biopsies were collected around the center of the skin. Bacteria obtained from the biopsy surface were collected by sterile swabbing (≥10 times) and mopped (≥20 times) thoroughly (with rotation of the swab) into a tube containing 1 ml of sterile PBS. The swab head with bacteria was cut off and dipped into the tube which was then vortexed thoroughly for 30 s. The number of viable bacteria (CFU/cm^2 of skin surface) was determined by serial dilution and drop plating. The lower limit of detection was 255 CFU/cm^2. To visualize the data on a logarithmic scale, a value of 255 CFU/cm^2 was assigned when no growth occurred. An additional 5-mm punch biopsy was also collected and then fixed in 10 % formalin, embedded in paraffin, sectioned (5 μm), and stained with hematoxylin and eosin (H&E stain) for histological examination. The stained sections were then imaged using a Zeiss Axioscope microscope.

2.9. MTS assay

CellTiter 96® AQueous One Solution Cell Proliferation (MTS) assay (Promega) was used to determine the viability of human dermal fibroblasts from adult (HDFa) (Lonza) when exposed to farnesol. Cells (5000/cm^2) were cultured with 200 μl of FGM™-2 fibroblast growth medium-2 BulletKit™ (Lonza) in a collagen-coated 96-well plate to form a monolayer (≥80 % of confluence) in a 37 °C, 5 % CO_2, humidified incubator. The medium was aspirated, cells were washed with 200 μl of PBS, and then incubated with 200 μl of medium containing 1, 6, or 15 mg/ml of farnesol. Cells were exposed to medium only, or medium containing the same amount of ethanol but without farnesol as medium and vehicle controls. After 24-hr incubation, the medium was aspirated, and the attached cells were washed with 200 μl of PBS, followed by the addition of 100 μl of MTS solution which had been diluted 1:4 with medium. The plate was incubated in the 37 °C, 5 % CO_2, humidified incubator for 2–4 h, while protected from light. The optical density at 490 nm was then measured using a TECAN Infinite M200 microplate reader with the MTS solution alone as a blank.

2.10. Statistical analysis

Data are expressed as the mean ± standard deviation of the mean unless stated otherwise. Statistical analysis of the data was performed using GraphPad Prism 9 (version 9.2.0). All statistical tests were two-sided. For analysis of the means of three or more groups, analysis of variance (ANOVA) tests were performed. In the event that ANOVA justified post hoc comparisons between group means, the comparisons were conducted using Tukey's multiple-comparisons test. Unpaired Student's t-test was used for comparisons between the means of two groups. The results were considered statistically significant at a value of $P < 0.05$.

3. Results

3.1. Farnesol inhibits biofilm formation of A. baumannii

We first evaluated the effect of farnesol against biofilm formation of *A. baumannii* type strain ATCC 19606 with multiple doses of farnesol treatments compared to their corresponding ethanol controls. 3 mg/ml of farnesol was found to be the optimal dose at inhibiting the biofilm formation without apparent vehicle (ethanol) killing, as indicated by about the 50-fold reduction of colony-forming units (CFU) (or about 98 % killing) (Fig. 1A). This result was further confirmed by dose response (up to 3 mg/ml) of farnesol on biofilm development of *A. baumannii* visualized by Live/Dead viability analysis (Fig. 1B), including quantitative analysis of fluorescence intensity using Photoshop® (Fig. 1C), and biomass and average biofilm thickness using Comstat2 (Fig. 1D). Farnesol was able to kill *A. baumannii* cells in a dose-dependent manner, and the resulting dead (red) cells seemed to barely attach the surfaces with the increase of farnesol doses (Fig. 1B–D) (this is why minimal red is observable in the images and the red signals detected by the software were much weaker than the green signals).

We also assessed the effect of farnesol against formation of

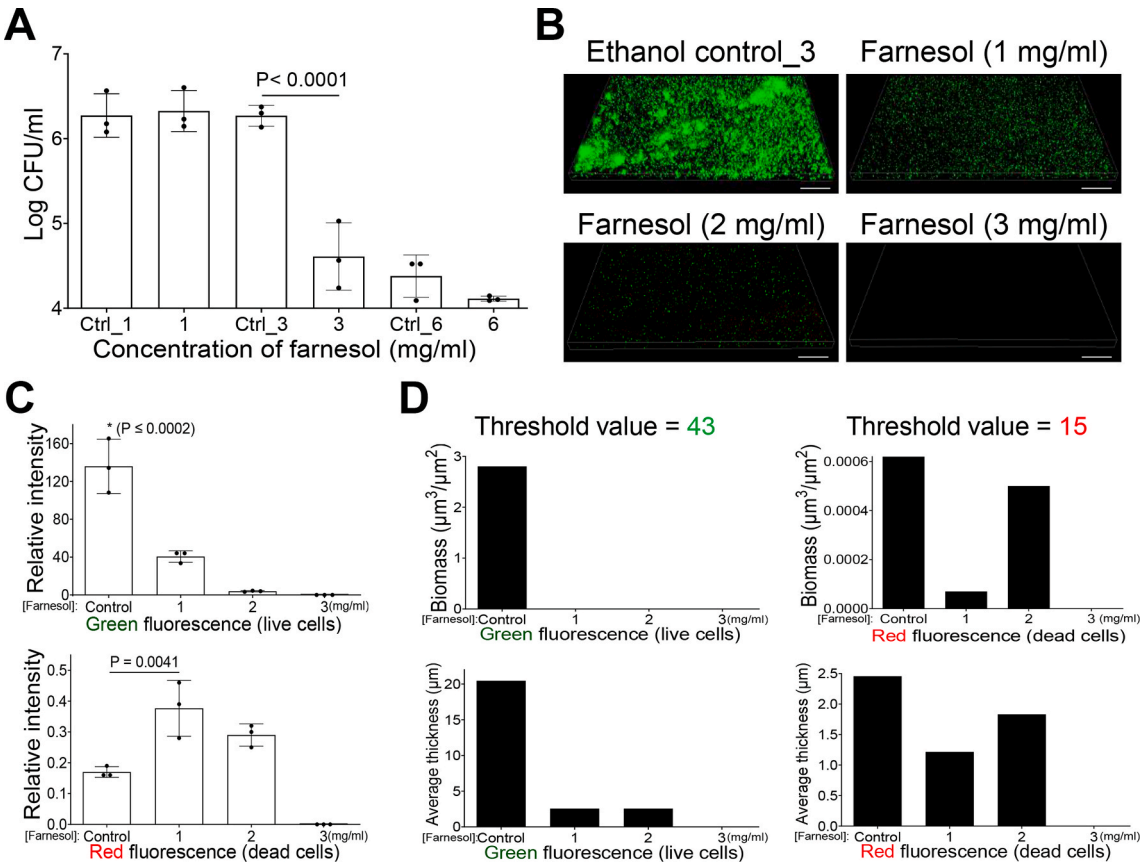

Fig. 1. Farnesol inhibits biofilm formation of *A. baumannii* type strain ATCC 19606. (**A**) Inhibition of biofilm formation of *A. baumannii* by farnesol 24 h after incubation in NB in plasma-coated wells. Results are expressed as the number of viable bacteria in log10 CFU per milliliter. Data are shown as mean ± standard deviation of the mean (SD) (n = 3). (**B**) Three-dimensional images of Live/Dead viability of *A. baumannii* biofilms after 24-h incubation in NB containing farnesol in plasma-coated chambers. Biofilms were stained with both SYTO® 9 (green fluorescence for live cells) and propidium iodide (red fluorescence for dead cells). Scale bars, 20 μm. (**C**) Quantitative analysis of relative fluorescence intensity in the biofilm images shown in (B) by Photoshop®. Data are shown as mean ± SD (n = 3). (**D**) Quantitative analysis of three-dimensional biofilm structure in the biofilm images shown in (B) by Comstat2, including biomass ($\mu m^3/\mu m^2$) and average thickness (μm). Threshold values for the analysis were set by Comstat2 using Otsu thresholding [54] in the images with the strongest green/red fluorescence and are shown at the top of the panels. The obtained threshold values were then applied to other images for fair comparison. Ctrl_# represents the vehicle (ethanol) control corresponding to the same amount of farnesol in ethanol. Ctrl_1 = 3.3 % of ethanol; Ctrl_3 = 10 % of ethanol; and Ctrl_6 = 20 % of ethanol. (For interpretation of the references to color in this figure legend, the reader is referred to the Web version of this article.)

A. baumannii BAA-1605 biofilms. This is a clinical strain showing multi-drug resistance [34]. Compared to the above *A. baumannii* ATCC 19606 results, farnesol is more effective at inhibiting biofilm formation of BAA-1605, as indicated by over 50-fold reduction of CFU at the low concentration (0.5 mg/ml) of farnesol (Fig. 2A). This result was also confirmed using Live/Dead viability evaluation of BAA-1605 biofilm development, and their corresponding quantitative analyses (Fig. 2B–D). Farnesol was capable of killing cells of BAA-1605 starting at a low dose of 0.1 mg/ml, causing an increase of dead (red) cells peaking at 0.2 mg/ml of farnesol by Photoshop® (Fig. 2C), or 0.5 mg/ml of farnesol by Comstat2 (as quantified by biomass) (Fig. 2D). This difference between the two analyses could be due to their distinct measurement principles: Photoshop® measures the overall fluorescence intensity of biofilms regardless their structure, whereas Comstat2 only analyzes biomass connected to the slide, thus excluding detached materials as biofilms [37]. Interestingly, farnesol was found to be highly effective to inhibit the biofilm formation of another clinical strain of *A. baumannii*, ATCC 17978, causing a 3000-fold CFU reduction when compared to its ethanol control (Fig. S2A), at the low concentration of 1 mg/ml.

3.2. Farnesol disrupts established biofilms of A. baumannii

Beside the inhibition of biofilm formation, farnesol also disrupted established biofilms of *A. baumannii* ATCC 19606, but requiring a higher concentration of farnesol at 10 mg/ml, which resulted in an over 70 % reduction of CFUs (Fig. 3A). This result was further confirmed by the viability analysis of ATCC 19606 established biofilms (Fig. 3B), and their corresponding quantitative analyses (Fig. 3C and D). As expected, there is a gradual decrease of live (green) biofilm-encased cells with the increase of farnesol doses. Unexpectedly, the intensity of red fluorescence was highest for the ethanol control (Fig. 3B–D). This could be due to that 1) the dead (red) biofilm-encased cells might rely on adjacent survival (green) cells for remaining on the surfaces, and 2) farnesol could remove/detach biofilm mass without killing (see below for biofilm detachment of farnesol).

The effect of farnesol against established biofilms of BAA-1605 was also examined. Farnesol at 6 mg/ml caused a greater than 1600-fold reduction of CFUs against the established BAA-1605 biofilms (Fig. 4A). This result suggests that farnesol has a stronger capacity for disrupting established biofilms of BAA-1605 compared to ATCC 19606. The Live/Dead viability analysis of established biofilms of BAA-1605 (Fig. 4B–D) further revealed that farnesol dose-dependently disrupted the established biofilms, resulting in a gradual decrease of live (green) biofilm-encased cells. Interestingly, red fluoresce for dead cells was peaking at 2 mg/ml of farnesol (Fig. 4C and D), suggesting that the dead (red) biofilm-encased cells seemed to be detached from the surfaces with the further increase of farnesol doses. As expected, farnesol (6 mg/ml)

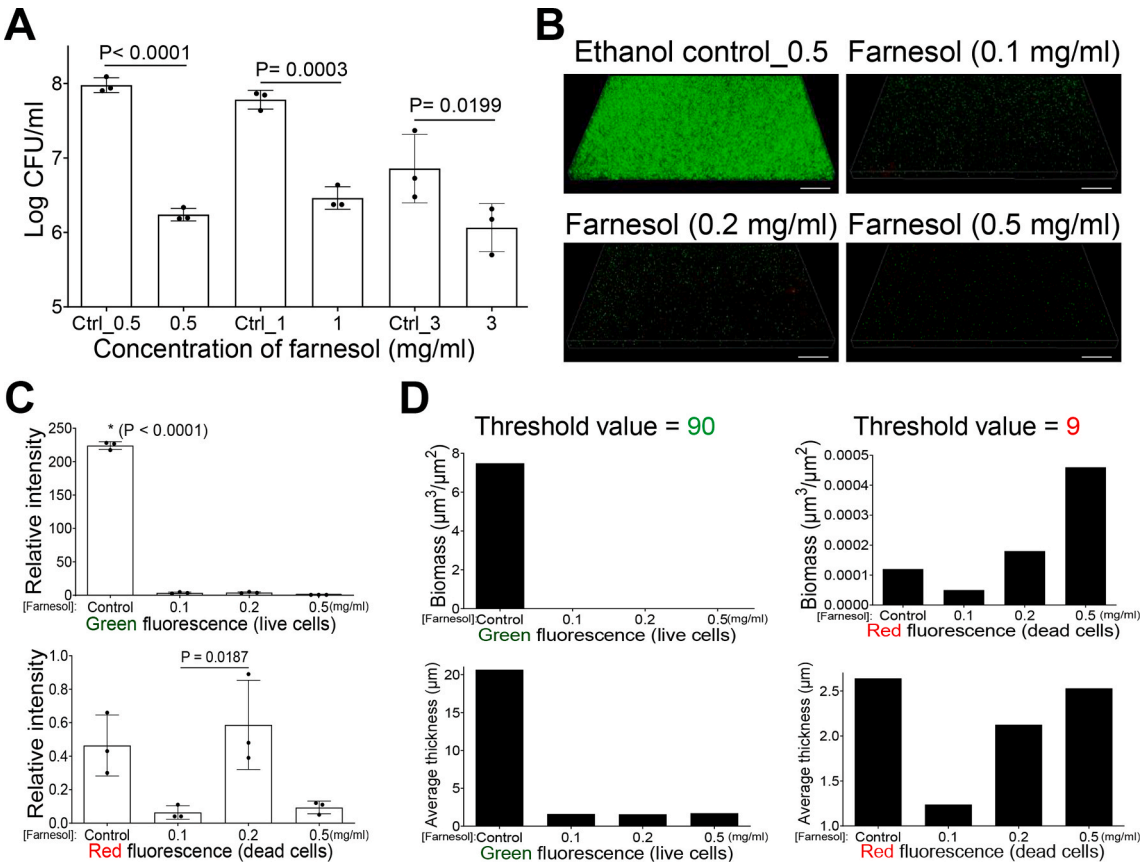

Fig. 2. Farnesol inhibits biofilm formation of *A. baumannii* clinic strain BAA-1605. (**A**) Inhibition of biofilm formation of BAA-1605 by farnesol 24 h after incubation in NB in plasma-coated wells. Results are expressed as the number of viable bacteria in log10 CFU per milliliter. Data are shown as mean ± SD (n = 3). (**B**) Three-dimensional images of Live/Dead viability of BAA-1605 biofilms after 24-h incubation in NB containing farnesol in plasma-coated chambers. Biofilms were stained with both SYTO® 9 (green fluorescence for live cells) and propidium iodide (red fluorescence for dead cells). Scale bars, 20 μm. (**C**) Quantitative analysis of relative fluorescence intensity in the biofilm images shown in (B) by Photoshop®. Data are shown as mean ± SD (n = 3). (**D**) Quantitative analysis of three-dimensional biofilm structure in the biofilm images shown in (B) by Comstat2, including biomass ($\mu m^3/\mu m^2$) and average thickness (μm). Threshold values of green and red fluorescence for the analysis are shown at the top of the panels. Ctrl_0.5 = 1.7 % of ethanol, Ctrl_1 = 3.3 % of ethanol; Ctrl_3 = 10 % of ethanol. (For interpretation of the references to color in this figure legend, the reader is referred to the Web version of this article.)

was also able to disrupt the established biofilms of *A. baumannii* ATCC 17978 with an even higher efficacy, resulting in an almost 4-log CFU reduction compared to its ethanol control (Fig. S2B).

Of note, for the above cases of biofilm formation and established biofilms, the effects of higher doses of farnesol on *A. baumannii* biofilms were masked due to the toxic effects of the vehicle (ethanol) at higher concentrations (Control_6 = 20 % of ethanol; Control_10 = 33 % of ethanol; Control_15 = 50 % of ethanol) (Figs. 1A–3A and 4A).

3.3. No resistance to farnesol was observed

Since development of antibiotic resistance is a challenge for *A. baumannii* infections [4], we evaluated the ability of *A. baumannii* ATCC 19606 to develop resistance to farnesol. Serial passaging of *A. baumannii* in the presence of sub-inhibitory [1/2 × minimal inhibitory concentration (MIC)] concentrations of farnesol did not select isolates resistant to farnesol, even after 20 continuous passages. In contrast, exposure to the antibiotic rifampicin elicited a swift increase in MIC after 13 passages, eventually resulting in a ≥8192-fold increase in MIC after 18 passages (Fig. 5A). These results demonstrate that no resistance to farnesol was observed even after prolonged culture in the presence of sub-inhibitory farnesol doses.

3.4. Farnesol kills A. baumannii and also detaches biofilms

The anti-biofilm effects of farnesol against *A. baumannii* can be best appreciated by exploring the mechanisms of action. Since farnesol has been shown to induce membrane disruption of *Staphylococcus aureus* [39], we wanted to evaluate whether farnesol kills *A. baumannii* by the same mechanism, which was accomplished using propidium iodide (PI) influx. Farnesol promoted PI influx in response to both the dose and time of exposure, with 10 mg/ml of farnesol showing the optimal effect (Fig. 5B), which is consistent to the above CFU data (Fig. 3A). As a negative control, the ethanol vehicle had no effect on the PI influx (Fig. 5B). This result indicates that farnesol is capable of killing the Gram-negative *A. baumannii* perhaps by disrupting the cell membrane, similar to what occurs in Gram-positive *S. aureus*.

It has also been proposed that farnesol can induce detachment of established *S. epidermidis* biofilms without cell killing [40]. The lack of red fluorescence in farnesol-treated established *A. baumannii* ATCC 19606 biofilms could also partially due to the potential biofilm detachment by farnesol. We evaluated biofilm detachment visually using Live/Dead viability analysis of *A. baumannii* detached cells, which were detached from the surface and entered into the supernatant following farnesol treatment of established biofilms. Interestingly, centrifugation of the detached cells formed no visible pellet for the ethanol control, but generated progressively looser (and more difficult to collect by centrifuging) pellets with the increase of farnesol doses (Fig. S3). Live/Dead viability analysis revealed that 3 mg/ml of farnesol elicited detachment of a live biofilm mass from the established biofilms, without cell killing (as indicated by the green fluorescence). Farnesol at a concentration of 6 mg/ml appeared to disintegrate the detached

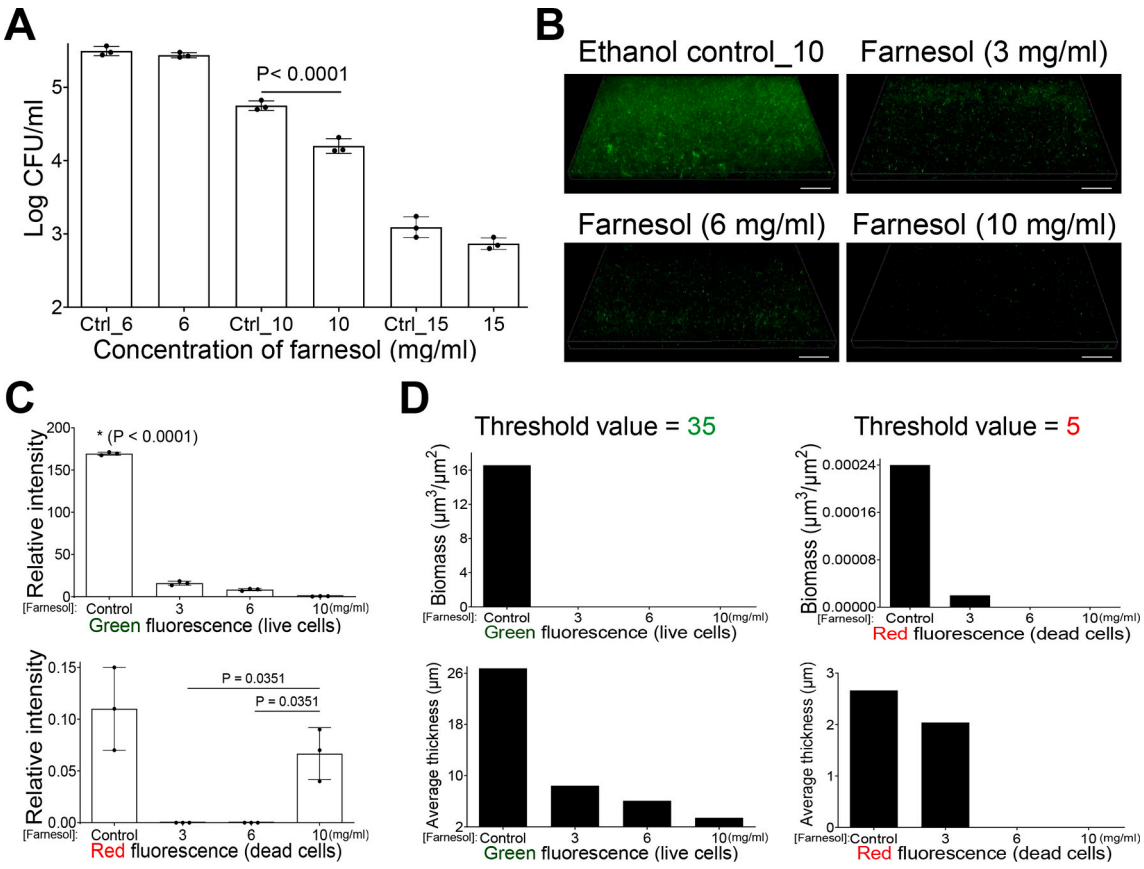

Fig. 3. Farnesol disrupts established biofilms of *A. baumannii* type strain ATCC 19606. (**A**) Disruption of established biofilms of *A. baumannii* by farnesol. Results are expressed as the number of viable bacteria in log10 CFU per milliliter after 24-h exposure of 24-h-old established biofilms to farnesol. Data are shown as mean ± SD (n = 3). (**B**) Three-dimensional images of Live/Dead viability of *A. baumannii* biofilms after 24-h exposure of 24-h-old established biofilms in NB containing farnesol in plasma-coated chambers. Biofilms were stained with both SYTO® 9 (green fluorescence for live cells) and propidium iodide (red fluorescence for dead cells). Scale bars, 20 μm. (**C**) Quantitative analysis of relative fluorescence intensity in the biofilm images shown in (B) by Photoshop®. Data are shown as mean ± SD (n = 3). (**D**) Quantitative analysis of three-dimensional biofilm structure in the biofilm images shown in (B) by Comstat2, including biomass ($\mu m^3/\mu m^2$) and average thickness (μm). Threshold values of green and red fluorescence for the analysis are shown at the top of the panels. Ctrl_6 = 20 % of ethanol; Ctrl_10 = 33.3 % of ethanol; and Ctrl_15 = 50 % of ethanol. (For interpretation of the references to color in this figure legend, the reader is referred to the Web version of this article.)

biofilm mass into small pieces. Ultimately, 10 mg/ml of farnesol demonstrated the capability of killing the detached cells (as indicated by red fluorescence) (Fig. 5C). Collectively, these results suggest that farnesol is bactericidal perhaps by cell membrane disruption, while also detaching biofilms from surfaces without killing at lower doses.

3.5. Farnesol is effective against biofilm-related skin infections

A. baumannii has been frequently isolated from the skin of patients with burns, wounds, or trauma [4]. Among patients with burns, patients with *A. baumannii* infection had more severe burns and comorbidities, longer lengths of stay, and higher mortality compared to patients without infection [41]. Thus, we sought to examine the efficiency of farnesol against *A. baumannii* biofilms developed on skin using *ex vivo* intact, or burned, human skin. Ethanol alone failed to kill *A. baumannii* ATCC 19606 on *ex vivo* human skin, which allowed higher doses of farnesol to be used (6 mg/ml for biofilm formation; 15 mg/ml for established biofilms) in the *ex vivo* study. Fresh human skin was inoculated with *A. baumannii* ATCC 19606 in the presence and absence of 6 mg/ml of farnesol for 24 h to evaluate its potential to inhibit biofilm development. Farnesol significantly inhibited *A. baumannii* biofilm formation on intact human skin, as visualized by a reduction of *A. baumannii* on top of the epidermis (Fig. 6A). This result was further confirmed by CFU reduction of *A. baumannii* on the skin (Fig. 6B). Similar results occurred for inhibiting *A. baumannii* biofilm formation on burned human skin (with ruptured epidermis due to burn wound creation) by the farnesol treatment (Fig. 6C and D). Hematoxylin and eosin (H&E) staining of the skin revealed that the established *A. baumannii* biofilm infection on intact human skin caused detachment of the epidermis (Compare both controls in Fig. 6A with Fig. 6E). In contrast, farnesol (15 mg/ml) provided observable protection from this epidermal damage (Fig. 6E). Farnesol's disruption of established biofilms of *A. baumannii* on the skin surface was further confirmed by significant decreases in CFUs (Fig. 6F). Furthermore, 15 mg/ml of farnesol was also effective against established *A. baumannii* biofilms on burned skin, as demonstrated by the substantial biofilm reduction on the epidermis (Fig. 6G), as well as a significant CFU reduction (Fig. 6H).

Since the *in-vitro* results show that farnesol is more effective for both inhibition of biofilm formation and disruption of established biofilms against the prevalent clinic strain *A. baumannii* BAA-1605 compared to ATCC 19606, we examined whether lower doses of farnesol are sufficient for both prevention and treatment of BAA-1605 biofilms on *ex vivo* intact, or burned human skin. Farnesol at 1 mg/ml inhibited BAA-1605 biofilm formation on intact human skin, as visualized by the decrease of BAA-1605 biofilms on the epidermal layer (Fig. 7A), and further confirmed by the 70–90 % reduction of CFUs (Fig. 7B). Similar results ensued for inhibition of BAA-1605 biofilm formation on burned human skin (Fig. 7C and D). The established BAA-1605 biofilms on intact human skin not only resulted in epidermal detachment, but also caused collapse of the underlying dermal layer (Fig. 7E). Farnesol's protection

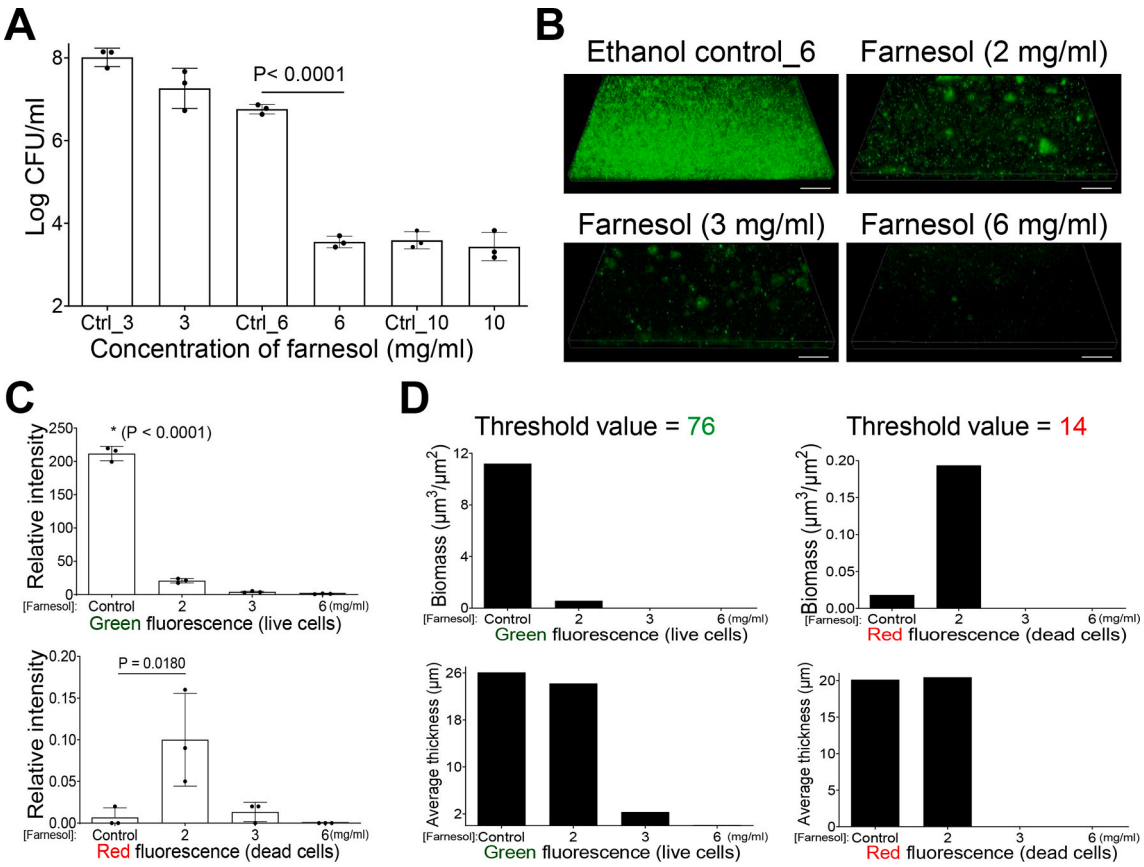

Fig. 4. Farnesol disrupts established biofilms of *A. baumannii* clinic strain BAA-1605. (**A**) Disruption of established biofilms of BAA-1605 by farnesol. Results are expressed as the number of viable bacteria in log10 CFU per milliliter after 24-h exposure of 24-h-old established biofilms to farnesol. Data are shown as mean ± SD (n = 3). (**B**) Three-dimensional images of Live/Dead viability of BAA-1605 biofilms after 24-h exposure of 24-h-old established biofilms in NB containing farnesol in plasma-coated chambers. Biofilms were stained with both SYTO® 9 (green fluorescence for live cells) and propidium iodide (red fluorescence for dead cells). Scale bars, 20 μm. (**C**) Quantitative analyses of relative fluorescence intensity in the biofilm images shown in (B) by Photoshop®. Data are shown as mean ± SD (n = 3). (**D**) Quantitative analyses of three-dimensional biofilm structure in the biofilm images shown in (B) by Comstat2, including biomass ($\mu m^3/\mu m^2$) and average thickness (μm). Threshold values of green and red fluorescence for the analyses are shown at the top of the panels. Ctrl_3 = 10 % of ethanol; Ctrl_6 = 20 % of ethanol; and Ctrl_10 = 33.3 % of ethanol. (For interpretation of the references to color in this figure legend, the reader is referred to the Web version of this article.)

of the biofilm-infected skin was demonstrated at 6 mg/ml, which prevented serious damage in both the epidermal and dermal layers, together with the observable biofilm reduction on the epidermis (Fig. 7E). We also detected substantial CFU reductions on the skin from two independent human samples using 6 mg/ml of farnesol (Fig. 7F). Similarly, farnesol at 6 mg/ml is also protective against damage caused by established BAA-1605 biofilms on burned skin, as observed by the biofilm decrease on top of the skin (Fig. 7G), as well as significant CFU reductions (Fig. 7H). The above results demonstrate that farnesol is effective for both prevention and treatment of biofilm-associated infections of *A. baumannii ex vivo*.

3.6. *Farnesol is safe ex vivo and protects HDFa from ethanol killing in vitro*

In consideration of safety, farnesol concentrations as high as 15 mg/ml had no observable side effects on *ex vivo* human intact skin over a 48-h culture period (Fig. S4). To further evaluate whether farnesol is safe for treatment of open-wound skin infections, MTS assay was used to assess potential cytotoxicity of farnesol/ethanol on HDFa, the cells within the dermis layer of skin playing a critical role in wound healing [42]. Although as low as 3.3 % of ethanol showed some toxicity to HDFa, farnesol is not toxic to HDFa, and appears to offer a protective benefit against ethanol toxicity. Among the three farnesol doses (1, 6, or 15 mg/ml), 6 mg/ml of farnesol showed the best outcome, although all of three doses are safe to HDFa (Fig. 8). These results strongly suggest that farnesol is safe for both prevention and treatment of intact or open-wound skin infections.

4. Discussion

Emergence of the superbug *A. baumannii* with resistance to last-resort antibiotics, along with its pervasive biofilm-associated infection, raises serious concerns for treatment failure of the formidable infections [43,44]. Here we show that farnesol, a FDA-approved GRAS compound, is effective for both prevention of biofilm formation, and also for disruption of established biofilms of *A. baumannii*, both *in vitro* and *ex vivo*. Furthermore, *A. baumannii* showed no sign of resistance development to farnesol, even after twenty continuous cultures in the presence of sub-MIC doses, which addresses the issue of antibiotic resistance.

We have shown that farnesol is able to kill *A. baumannii* cells perhaps by disrupting cell membranes, in addition to its potential to detach biofilms from surfaces at sub-lethal doses. This anti-biofilm mechanism gives farnesol multiple advantages for combating *A. baumannii* infections: 1) to kill the superbug directly, thus eliminating future recurrence, and 2) to detach biofilms from surfaces/tissues at low doses that are harmless to the host or environment. The mechanism by which farnesol detaches biofilms without killing is not yet known. However, farnesol has been shown capable of dissolving fibrin fibers of established biofilms of *S. aureus* [31]. Interestingly, *A. baumannii* was recently found to rely on adhesive, extracellular fibers for biofilm formation in catheter-associated urinary tract infections [45]. The potential fiber

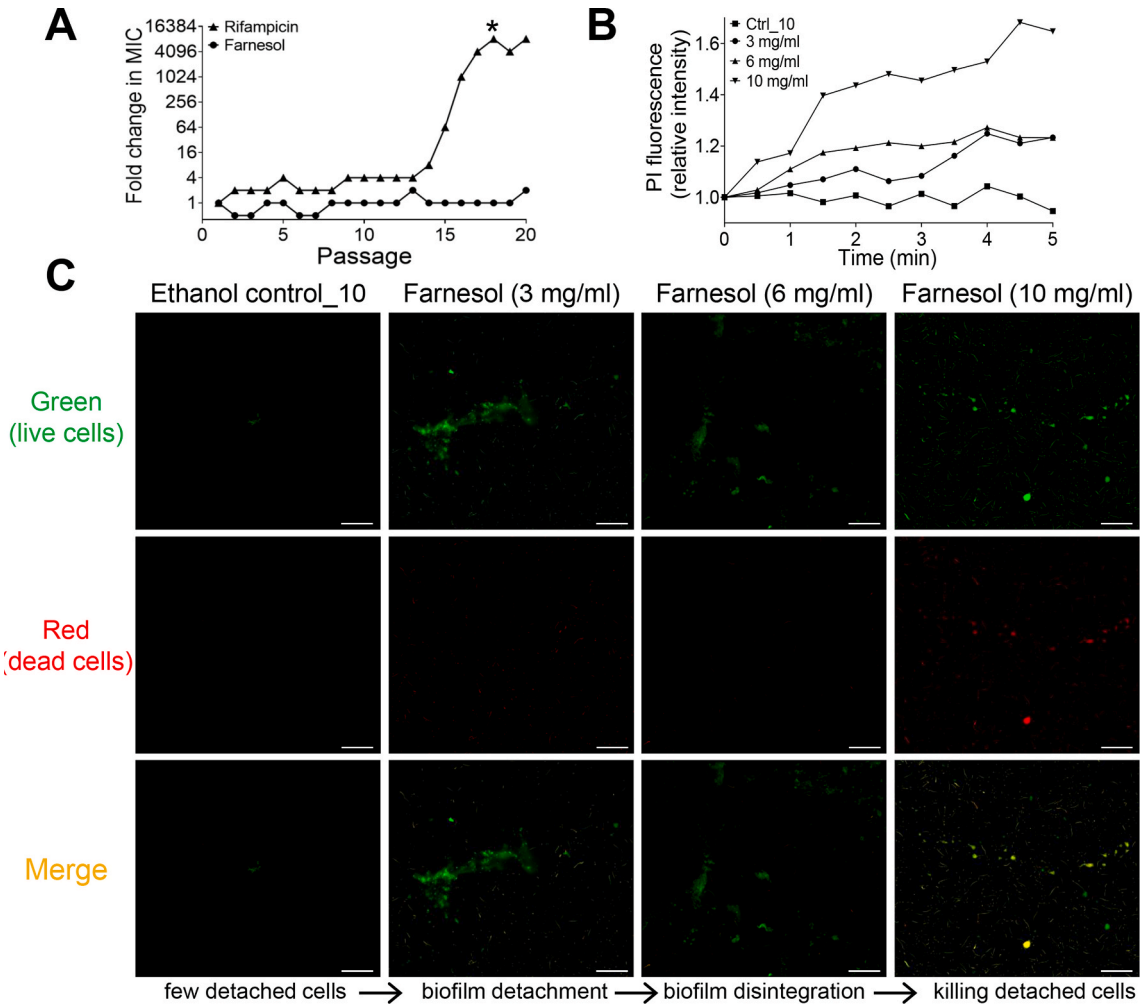

Fig. 5. Farnesol combats *A. baumannii* without inducing resistance by direct killing and biofilm detachment. (**A**) Resistance development of *A. baumannii* to farnesol, or the antibiotic rifampicin, respectively, during serial passaging in the presence of sub-minimal inhibitory concentration (MIC) levels of antimicrobials. Data are fold changes (in log2) in MIC relative to the MIC of the first passage (1 mg/ml for farnesol; 4 μg/ml for rifampicin). * Bacteria remained growing in the highest concentration (16 mg/ml) of rifampicin stock so that the MIC was assumed to be ≥ 32 mg/ml. (**B**) Killing of *A. baumannii* by farnesol as measured by propidium iodide (PI) influx. Data were normalized to the ethanol control at time zero and are shown as the mean of three replicates. (**C**) Biofilm detachment, disintegration, and killing of *A. baumannii* after 24-h exposure of established biofilms to farnesol as measured by Live/Dead viability assay. The supernatant containing detached bacteria after farnesol treatment were centrifuged, and the obtained pellet was then washed and stained with both SYTO® 9 (green fluorescence for live cells) and PI (red fluorescence for dead cells). The obtained green, red, and merged signals were displayed side-by-side. Scale bars, 20 μm. Ctrl_10 = 33.3 % of ethanol. (For interpretation of the references to color in this figure legend, the reader is referred to the Web version of this article.)

breakage by farnesol against *A. baumannii* might elicit biofilm detachment and disintegration, as visualized in Fig. 5C.

The mechanisms by which farnesol escapes development of resistance remains mysterious. *A. baumannii* has been known to acquire resistance to various antibiotics by changing target sites, reducing intracellular accumulation, and by enzymatic modification causing antibiotic neutralization [46]. Since these resistance mechanisms require participation of a mutant protein/enzyme, it is possible that farnesol might permeabilize bacterial cell membranes from the outside without any protein participation so that a potential protein mutation would not have an effect, similar to the effects of antimicrobial peptides [38].

A. baumannii is a well-known pathogen isolated from burns and wounds [4,47]. We have shown that farnesol is effective in combating biofilm infections of three *A. baumannii* stains: the type strain ATCC 19606 (drug sensitive), a clinical strain that is also drug sensitive (ATCC 17978), and the clinical strain BAA-1605, that is MDR. Interestingly, compared to the type strain, farnesol is more effective against the BAA-1605 biofilm infections both *in vitro* and *ex vivo*, and at lower doses. Our results contrast those of previous works which have shown that farnesol was not effective against MDR strains of *A. baumannii* and highlight that susceptibility to farnesol is strain dependent [24]. Since *A. baumannii* BAA-1605 is a battlefield-originating strain showing multi-drug resistance, and *A. baumannii* currently represents the biggest threat for military personnel with war wounds/burns [48], our finding that farnesol is highly effective for preventing and treating *A. baumannii* BAA-1605 biofilm infections will have significant clinic importance.

Farnesol is an FDA-approved GRAS compound, and concentrations up to 120 mg/ml have been proven to be safe on human skin as a fragrance ingredient [14]. Consistent with this, we revealed that up to 15 mg/ml of farnesol in ethanol was safe without any damage in an *ex vivo* human skin model. Moreover, we demonstrated that up to 15 mg/ml of farnesol is not only safe to HDFa, but also protects HDFa from apparent ethanol killing *in vitro*. The reason why farnesol may protect the fibroblasts from damage might be because that farnesol is oily, it creates an emulsion when the farnesol stock (30 mg/ml) in ethanol was diluted with aqueous media, which may sequester ethanol within a farnesol capsule, thereby negating ethanol toxicity. Furthermore, farnesol is low-cost (about $1 per gram from Sigma) compared with most commercial antibiotics. Collectively, these results suggest that topical

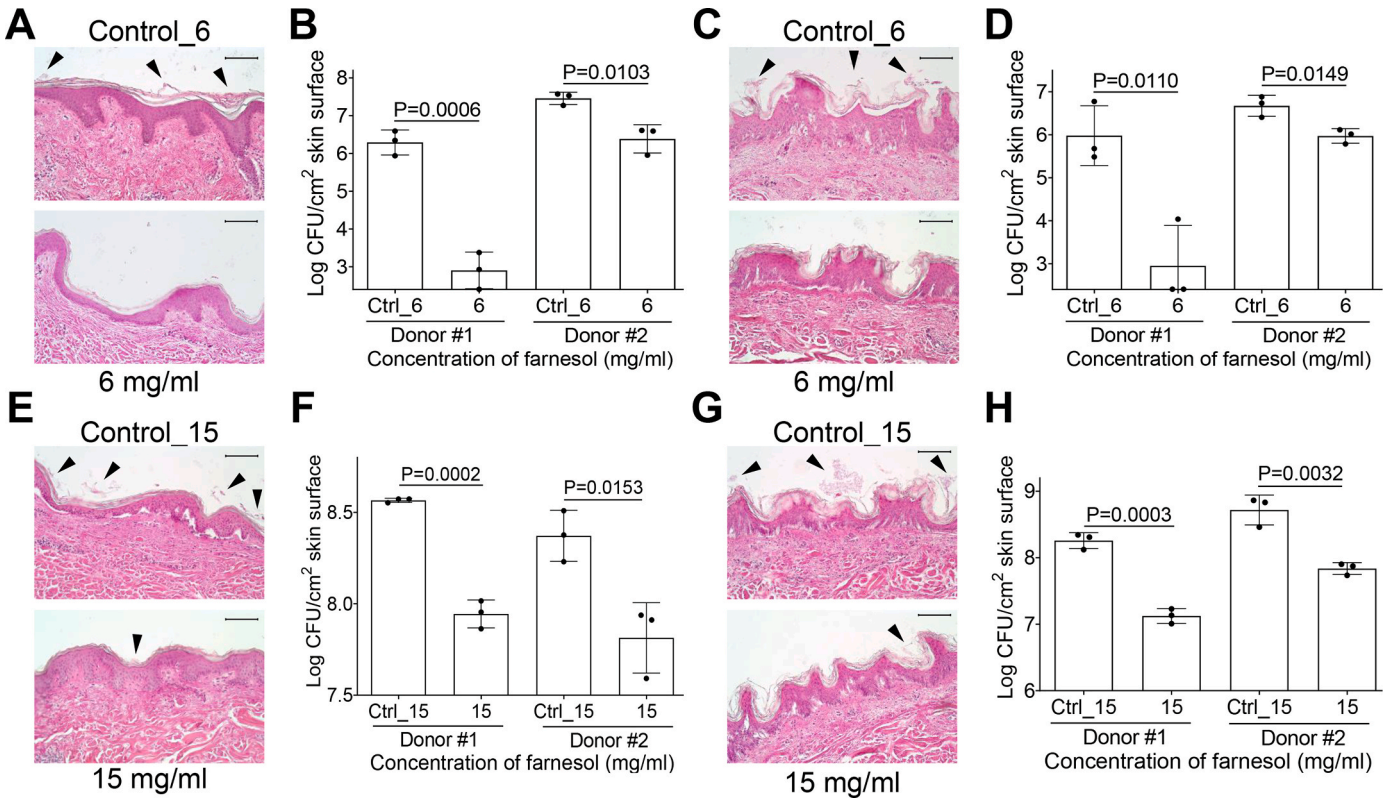

Fig. 6. Farnesol is effective for both prevention and treatment of biofilm-associated infections of *A. baumannii* ATCC 19606 on an *ex vivo* intact or burned human skin. (A and **B)** Prevention of biofilm formation of *A. baumannii* by farnesol (6 mg/ml) 24 h after inoculation on *ex vivo* intact human skin as assayed by light micrographs of hematoxylin and eosin (H&E)-stained crossing sections of skin biopsies (A), and vital cell counts expressed as the number of viable bacteria in $\log_{10}$ CFU per square centimeter (cm^2) of skin (B). **(C** and **D)** Prevention of biofilm-associated infections of *A. baumannii* by farnesol (6 mg/mL) 24 h after inoculation on *ex vivo* burned human skin as assayed by light micrographs of H&E-stained crossing sections of skin biopsies (C), and vital cell counts expressed as the number of viable bacteria in $\log_{10}$ CFU/cm^2 of skin (D). **(E** and **F)** Farnesol protection from epidermal detachment and alleviation of established *A. baumannii* biofilms after 24-h inoculation followed by 24-h exposure to farnesol (15 mg/mL) on *ex vivo* intact human skin, as assayed by light micrographs of H&E-stained cross-sections of skin biopsies (E), and vital cell counts expressed as the number of viable bacteria in $\log_{10}$ CFU/cm^2 of skin (F). **(G** and **H)** Mitigation of established *A. baumannii* biofilms after 24-h inoculation followed by 24-h exposure to farnesol (15 mg/mL) on *ex vivo* burned human skin, as assayed by light micrographs of H&E-stained cross-sections of skin biopsies (G), and vital cell counts expressed as the number of viable bacteria in $\log_{10}$ CFU/cm^2 of skin (H). Arrowheads in (A, C, E, and G) indicate biofilm formation or establishment on skin. (B, D, F, and H) Data are shown as mean ± SD (n = 3) from two independent donors/experiments. The X-axis line in (B and D) represents the lower limit of detection (Log 255 ≈ 2.4). Ctrl_6 = 20 % of ethanol and Ctrl_15 = 50 % of ethanol.

application of farnesol may be promising as an affordable and effective treatment of *A. baumannii*-associated wound/burn infections, such as farnesol-related topical formulations and wound dressings.

Drug repurposing has recently received increasing attention as an alternative approach to rapidly identify drugs and drug combinations to combat MDR *A. baumannii* infections [49]. As a result, some unconventional drugs have been screened *in vitro* as promising candidates for repurposing, including apramycin, mitomycin C, 5-fluorouracil, fusidic acid, niclosamide, phenothiazine derivatives and fluspirilene, amongst others [49–52]. However, due to high toxicity of manyagents (with some being potent antitumoral and DNA damaging agents) and low plasma concentrations in patients, their potential clinical applicability had been restricted [49]. In addition, teams have sought the potential use of farnesol as an adjuvant to antibiotics [23]. Although drug combinations might reduce the emergence of antimicrobial resistance, heteroresistance of *A. baumannii* against multiple drugs is still a concern due to its apparently endless capacity to acquire antibiotic resistance [49]. Our results have demonstrated, for the first time, that farnesol alone (when dissolved in ethanol then diluted in aqueous media to form an emulsion) is an effective, safe, and affordable solution to combat biofilm infections of *A. baumannii.* Furthermore, bacterial resistance to farnesol seems not to occur to *A. baumannii.*

The current study has provided a proof of concept that farnesol alone is an unexpected but effective agent against *A. baumannii* biofilm-associated infections, but it has some limitations. First, due to limited availability of *ex vivo* human skin, we were only able to test one dose at one time point (24 h after treatment). A higher farnesol dose (e.g. > 6 mg/ml in Fig. 6B) and/or a longer treatment time might produce better results. Secondly, we used a previously established protocol to examine the resistance development of farnesol compared to rifampicin, with rifampicin resistance being seen at passage 13 and hence we only maintained up to passage 20. Although we did not observe resistance to farnesol after 20 passages, we could not rule out the possibility that additional (e.g., up to 50 or more) passages might show resistance to farnesol, Thirdly, although we employed the vehicle (ethanol) controls throughout our experiments, ethanol on its own has an antimicrobial effect, although in many places the effect of farnesol becomes apparent and is superior to ethanol alone. Alcohol is often applied to the skin at 100 %, albeit quickly, as an antiseptic. Low doses of ethanol are needed to carry farnesol and inhibit biofilm development (up to 10 %) whereas higher doses of ethanol used to carry farnesol (up to 33.3 %) are needed to disrupt established biofilms. These doses are quite moderate. Since the antimicrobial effect of farnesol appears to occur rapidly, we envision that farnesol in ethanol could be applied quickly to the skin for improved antimicrobial effect compared to alcohol alone. Although 50 % ethanol was used to examine the impact of 15 mg/ml of farnesol, this dose was only needed against one strain of *A. baumannii*, ATCC 19606. Interestingly, there was no benefit of farnesol compared to ethanol at 50 % for

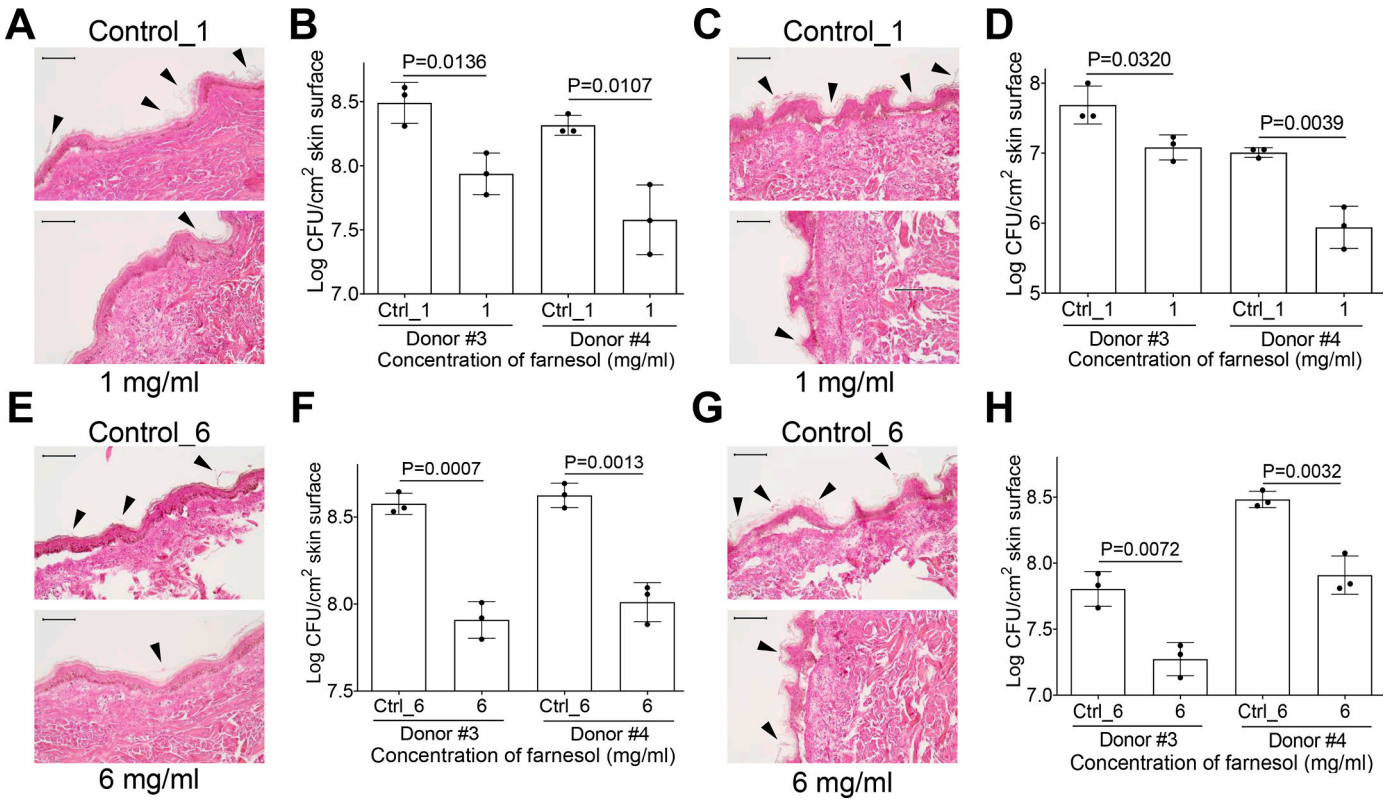

Fig. 7. Farnesol is effective for both prevention and treatment of biofilm-associated infections of *A. baumannii* BAA-1605 on an *ex vivo* intact or burned human skin. (A and **B)** Prevention of BAA-1605 biofilm formation by farnesol (1 mg/ml) 24 h after inoculation on *ex vivo* intact human skin as assayed by light micrographs of H&E-stained crossing sections of skin biopsies (A), and vital cell counts expressed as the number of viable bacteria in $\log_{10}$ CFU/cm^2 of skin (B). **(C** and **D)** Prevention of BAA-1605 biofilms by farnesol (1 mg/ml) 24 h after inoculation on *ex vivo* burned human skin as assayed by light micrographs of H&E-stained crossing sections of skin biopsies (C), and vital cell counts expressed as the number of viable bacteria in $\log_{10}$ CFU/cm^2 of skin (D). **(E** and **F)** Farnesol protection from epidermal detachment and dermal collapse, as well as mitigation of established BAA-1605 biofilms after 24-h inoculation followed by 24-h exposure to farnesol (6 mg/ml) on *ex vivo* intact human skin, as assayed by light micrographs of H&E-stained cross-sections of skin biopsies (E), and vital cell counts expressed as the number of viable bacteria in $\log_{10}$ CFU/cm^2 of skin (F). **(G** and **H)** Farnesol protection from severe skin damage of both the epidermal and dermal layers, as well as alleviation of established BAA-1605 biofilms after 24-h inoculation followed by 24-h exposure to farnesol (6 mg/ml) on *ex vivo* burned human skin, as assayed by light micrographs of H&E-stained cross-sections of skin biopsies (G), and vital cell counts expressed as the number of viable bacteria in $\log_{10}$ CFU/cm^2 of skin (**H**). Arrowheads in (A, C, E, and G) indicate biofilm formation or establishment on skin. (B, D, F, and H) Data are shown as mean ± SD (n = 3) from two additional independent donors/experiments. Ctrl_1 = 3.3 % of ethanol and Ctrl_6 = 20 % of ethanol.

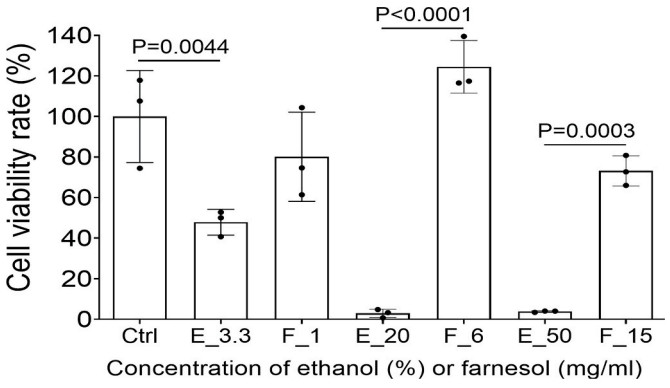

Fig. 8. Farnesol is not toxic and further protects HDFa from apparent ethanol killing. Potential cytotoxicity of three farnesol doses (1, 6, 15 mg/ml) and their corresponding vehicle (ethanol) controls on HDFa monolayers was evaluated by MTS assay. Ctrl, Media control; E_# represents the ethanol percentage (%) in vehicle control; F_# represents the farnesol concentrations in the unit of mg/ml.

the ATCC 19606 strain *in vitro* against established biofilm. However, as shown in Fig. 6, farnesol in 50 % of ethanol (15 mg/ml) is superior to ethanol alone for reducing viable bacteria in intact or burned human skin. Additionally, only 1.7 % and 20 % ethanol was needed to carry farnesol for effective reduction of biofilm development or biofilm disruption for the MDR strain BAA-1605, respectively. This result supports our position that farnesol in ethanol, when it can be carried at high concentration, such as it can be in ethanol, confers a protective benefit. It is worth mentioning that farnesol has also been approved as a food ingredient by FDA. Since the high doses (6 or 15 mg/ml) of farnesol have been shown to protect HDFa from ethanol killing by the MTS assay, the potential application of farnesol for internal clinical use could also be possible. Future study will address the issue of multiple farnesol doses and treatment time points and the feasibility of extending farnesol's clinical applications from topical delivery to internal medical use (e.g. farnesol-embedded coatings or implants).

In conclusion, we have demonstrated that farnesol is a prospective candidate for both prevention and treatment of *A. baumannii* biofilms due to its established safety, low-cost, topical delivery, and excellent efficiency, along with the capacity to impede development of therapeutic resistance. Currently available treatments for MDR *A. baumannii* infections rely on the delicate combinations of last-resort antibiotics [53]. Thus, innovative strategies against *A. baumannii* infections are urgently desirable. Repurposing of farnesol as a single agent for both prevention and treatment of MDR *A. baumannii*-associated biofilm infections represents a ground-breaking strategy to combat this notorious superbug.

Competing interests

The authors declare competing financial interests.

CRediT authorship contribution statement

Li Tan: Writing – original draft, Methodology, Investigation, Formal analysis, Data curation, Conceptualization. **Rong Ma:** Investigation. **Adam J. Katz:** Writing – review & editing, Supervision, Funding acquisition. **Nicole Levi:** Writing – review & editing, Supervision, Conceptualization.

Declaration of competing interest

The authors declare competing financial interests. We (LT, AJK, and NL) have filed a provisional patent application related to work in this paper.

Data availability

Data will be made available on request.

Acknowledgments

We thank Dr. Ramon Llull for discussions and technical support on the Keyence® fluorescence microscope. This work was supported by internal funding from the Department of Plastic and Reconstructive Surgery at Wake Forest University School of Medicine.

Appendix A. Supplementary data

Supplementary data to this article can be found online at https://doi.org/10.1016/j.bioflm.2024.100198.

References

[1] Mulani MS, Kamble EE, Kumkar SN, Tawre MS, Pardesi KR. Emerging strategies to combat eskape pathogens in the era of antimicrobial resistance: a review. Front Microbiol 2019;10.
[2] De Silva PM, Chong P, Fernando DM, Westmacott G, Kumar A. Effect of incubation temperature on antibiotic resistance and virulence factors of *Acinetobacter baumannii* ATCC 17978. Antimicrob Agents Chemother 2017;62:e01514. https://doi.org/10.1128/AAC.01514-17. 17.
[3] Peleg AY, Seifert H, Paterson DL. *Acinetobacter baumannii*: emergence of a successful pathogen. Clin Microbiol Rev 2008;21:538–82. https://doi.org/10.1128/CMR.00058-07.
[4] Ayoub Moubareck C, Hammoudi Halat D. Insights into *Acinetobacter baumannii*: a review of microbiological, virulence, and resistance traits in a threatening nosocomial pathogen. Antibiotics 2020;9:119. https://doi.org/10.3390/antibiotics9030119.
[5] Morris FC, Dexter C, Kostoulias X, Uddin MI, Peleg AY. The mechanisms of disease caused by *Acinetobacter baumannii*. Front Microbiol 2019;10.
[6] Nichols L. Death from pan-resistant superbug. Autopsy Case Rep 2019;9:e2019106. https://doi.org/10.4322/acr.2019.106.
[7] Zolnikov TR. Global health in action against a superbug. Am J Public Health 2019;109:523–4. https://doi.org/10.2105/AJPH.2019.304980.
[8] Vrancianu CO, Gheorghe I, Czobor IB, Chifiriuc MC. Antibiotic resistance profiles, molecular mechanisms and innovative treatment strategies of *Acinetobacter baumannii*. Microorganisms 2020;8:935. https://doi.org/10.3390/microorganisms8060935.
[9] Tacconelli E, Carrara E, Savoldi A, Harbarth S, Mendelson M, Monnet DL, et al. Discovery, research, and development of new antibiotics: the WHO priority list of antibiotic-resistant bacteria and tuberculosis. Lancet Infect Dis 2018;18:318–27. https://doi.org/10.1016/S1473-3099(17)30753-3.
[10] Costerton JW, Stewart PS, Greenberg EP. Bacterial biofilms: a Common cause of persistent infections. Science 1999;284:1318–22. https://doi.org/10.1126/science.284.5418.1318.
[11] Davies D. Understanding biofilm resistance to antibacterial agents. Nat Rev Drug Discov 2003;2:114–22. https://doi.org/10.1038/nrd1008.
[12] Ku C-M, Lin J-Y. Farnesol, a sesquiterpene alcohol in essential oils, ameliorates serum allergic antibody titres and lipid profiles in ovalbumin-challenged mice. Allergol Immunopathol 2016;44:149–59. https://doi.org/10.1016/j.aller.2015.05.009.
[13] de Araújo Delmondes G, Bezerra DS, de Queiroz Dias D, de Souza Borges A, Araújo IM, Lins da Cunha G, et al. Toxicological and pharmacologic effects of farnesol (C15H26O): a descriptive systematic review. Food Chem Toxicol 2019;129:169–200. https://doi.org/10.1016/j.fct.2019.04.037.
[14] Lapczynski A, Bhatia SP, Letizia CS, Api AM. Fragrance material review on farnesol. Food Chem Toxicol 2008;46:S149–56. https://doi.org/10.1016/j.fct.2008.06.046.
[15] Burdock GA. Fenaroli's handbook of flavor ingredients. sixth ed. Boca Raton: CRC Press; 2009. https://doi.org/10.1201/9781439847503.
[16] Ramage G, Saville SP, Wickes BL, López-Ribot JL. Inhibition of *Candida albicans* biofilm formation by farnesol, a quorum-sensing molecule. Appl Environ Microbiol 2002;68:5459–63. https://doi.org/10.1128/AEM.68.11.5459-5463.2002.
[17] Fernandes RA, Monteiro DR, Arias LS, Fernandes GL, Delbem ACB, Barbosa DB. Biofilm formation by *Candida albicans* and *Streptococcus mutans* in the presence of farnesol: a quantitative evaluation. Biofouling 2016;32:329–38. https://doi.org/10.1080/08927014.2016.1144053.
[18] Lee JH, Kim C, Kim S-H, Sethi G, Ahn KS. Farnesol inhibits tumor growth and enhances the anticancer effects of bortezomib in multiple myeloma xenograft mouse model through the modulation of STAT3 signaling pathway. Cancer Lett 2015;360:280–93. https://doi.org/10.1016/j.canlet.2015.02.024.
[19] Szűcs G, Murlasits Z, Török S, Kocsis GF, Pálóczi J, Görbe A, et al. Cardioprotection by farnesol: role of the mevalonate pathway. Cardiovasc Drugs Ther 2013;27:269–77. https://doi.org/10.1007/s10557-013-6460-2.
[20] Vinholes J, Rudnitskaya A, Gonçalves P, Martel F, Coimbra MA, Rocha SM. Hepatoprotection of sesquiterpenoids: a quantitative structure–activity relationship (QSAR) approach. Food Chem 2014;146:78–84. https://doi.org/10.1016/j.foodchem.2013.09.039.
[21] Jo A, Lee Y, Kam T-I, Kang S-U, Neifert S, Karuppagounder SS, et al. PARIS farnesylation prevents neurodegeneration in models of Parkinson's disease. Sci Transl Med 2021;13:eaax8891. https://doi.org/10.1126/scitranslmed.aax8891.
[22] Lopes AP, de Oliveira Castelo Branco RR, de Alcântara Oliveira FA, Campos MAS, de Carvalho Sousa B, Agostinho ÍRC, et al. Antimicrobial, modulatory, and antibiofilm activity of tt-farnesol on bacterial and fungal strains of importance to human health. Bioorg Med Chem Lett 2021;47:128192. https://doi.org/10.1016/j.bmcl.2021.128192.
[23] Han Y, Zhang Y, Zeng W, Huang Z, Cheng H, Kong J, et al. Synergy with farnesol rejuvenates colistin activity against Colistin-resistant Gram-negative bacteria in vitro and in vivo. Int J Antimicrob Agents 2023;62:106899. https://doi.org/10.1016/j.ijantimicag.2023.106899.
[24] Kostoulias X, Murray GL, Cerqueira GM, Kong JB, Bantun F, Mylonakis E, et al. Impact of a cross-kingdom signaling molecule of *Candida albicans* on *Acinetobacter baumannii* physiology. Antimicrob Agents Chemother 2015;60:161–7. https://doi.org/10.1128/aac.01540-15.
[25] Kaneko M, Togashi N, Hamashima H, Hirohara M, Inoue Y. Effect of farnesol on mevalonate pathway of *Staphylococcus aureus*. J Antibiot (Tokyo) 2011;64:547–9. https://doi.org/10.1038/ja.2011.49.
[26] Li W-R, Zeng T-H, Xie X-B, Shi Q-S, Li C-L. Inhibition of the pqsABCDE and pqsH in the pqs quorum sensing system and related virulence factors of the *Pseudomonas aeruginosa* PAO1 strain by farnesol. Int Biodeterior Biodegrad 2020;151:104956. https://doi.org/10.1016/j.ibiod.2020.104956.
[27] Gomes FIA, Teixeira P, Azeredo J, Oliveira R. Effect of farnesol on planktonic and biofilm cells of *Staphylococcus epidermidis*. Curr Microbiol 2009;59:118–22. https://doi.org/10.1007/s00284-009-9408-9.
[28] Pammi M, Liang R, Hicks JM, Barrish J, Versalovic J. Farnesol decreases biofilms of *Staphylococcus epidermidis* and exhibits synergy with nafcillin and vancomycin. Pediatr Res 2011;70:578–83. https://doi.org/10.1203/PDR.0b013e318232a984.
[29] Kuroda M, Nagasaki S, Ohta T. Sesquiterpene farnesol inhibits recycling of the C55 lipid carrier of the murein monomer precursor contributing to increased susceptibility to β-lactams in methicillin-resistant *Staphylococcus aureus*. J Antimicrob Chemother 2007;59:425–32. https://doi.org/10.1093/jac/dkl519.
[30] Jabra-Rizk MA, Meiller TF, James CE, Shirtliff ME. Effect of farnesol on *Staphylococcus aureus* biofilm formation and antimicrobial susceptibility. Antimicrob Agents Chemother 2006;50:1463–9. https://doi.org/10.1128/AAC.50.4.1463-1469.2006.
[31] Masako K, Hideyuki I, Shigeyuki O, Zenro I. A novel method to control the balance of skin microflora: Part 1. Attack on biofilm of *Staphylococcus aureus* without antibiotics. J Dermatol Sci 2005;38:197–205. https://doi.org/10.1016/j.jdermsci.2005.01.006.
[32] Hassan Abdel-Rhman S, Mostafa El-Mahdy A, El-Mowafy M. Effect of tyrosol and farnesol on virulence and antibiotic resistance of clinical isolates of *Pseudomonas aeruginosa*. BioMed Res Int 2015;2015:e456463. https://doi.org/10.1155/2015/456463.
[33] Zhu Y, Lu J, Zhao J, Zhang X, Yu HH, Velkov T, et al. Complete genome sequence and genome-scale metabolic modelling of *Acinetobacter baumannii* type strain ATCC 19606. Int J Med Microbiol IJMM 2020;310:151412. https://doi.org/10.1016/j.ijmm.2020.151412.
[34] Chopra S, Torres-Ortiz M, Hokama L, Madrid P, Tanga M, Mortelmans K, et al. Repurposing FDA-approved drugs to combat drug-resistant *Acinetobacter baumannii*. J Antimicrob Chemother 2010;65:2598–601. https://doi.org/10.1093/jac/dkq353.
[35] Herigstad B, Hamilton M, Heersink J. How to optimize the drop plate method for enumerating bacteria. J Microbiol Methods 2001;44:121–9. https://doi.org/10.1016/S0167-7012(00)00241-4.
[36] Heydorn A, Nielsen AT, Hentzer M, Sternberg C, Givskov M, Ersbøll BK, et al. Quantification of biofilm structures by the novel computer program comstat. Microbiology 2000;146:2395–407. https://doi.org/10.1099/00221287-146-10-2395.

[37] Vorregaard M. Comstat2 - a modern 3D image analysis environment for biofilms. Inform. Math. Model.. Kongens Lyngby, Denmark: Technical University of Denmark; 2008.
[38] de Breij A, Riool M, Cordfunke RA, Malanovic N, de Boer L, Koning RI, et al. The antimicrobial peptide SAAP-148 combats drug-resistant bacteria and biofilms. Sci Transl Med 2018;10:eaan4044. https://doi.org/10.1126/scitranslmed.aan4044.
[39] Inoue Y, Togashi N, Hamashima H. Farnesol-induced disruption of the *Staphylococcus aureus* cytoplasmic membrane. Biol Pharm Bull 2016;39:653–6. https://doi.org/10.1248/bpb.b15-00416.
[40] Cerca N, Gomes F, Bento JC, França A, Rolo J, Miragaia M, et al. Farnesol induces cell detachment from established *S. epidermidis* biofilms. J Antibiot (Tokyo) 2013; 66:255–8. https://doi.org/10.1038/ja.2013.11.
[41] Albrecht MA, Griffith ME, Murray CK, Chung KK, Horvath EE, Ward JA, et al. Impact of *acinetobacter* infection on the mortality of burn patients. J Am Coll Surg 2006;203:546–50. https://doi.org/10.1016/j.jamcollsurg.2006.06.013.
[42] Stunova A, Vistejnova L. Dermal fibroblasts—a heterogeneous population with regulatory function in wound healing. Cytokine Growth Factor Rev 2018;39: 137–50. https://doi.org/10.1016/j.cytogfr.2018.01.003.
[43] Sarshar M, Behzadi P, Scribano D, Palamara AT, Ambrosi C. *Acinetobacter baumannii:* an ancient commensal with weapons of a pathogen. Pathogens 2021;10: 387. https://doi.org/10.3390/pathogens10040387.
[44] Whiteway C, Breine A, Philippe C. Henst CV der. *Acinetobacter baumannii.* Trends Microbiol 2022;30:199–200. https://doi.org/10.1016/j.tim.2021.11.008.
[45] Tamadonfar KO, Di Venanzio G, Pinkner JS, Dodson KW, Kalas V, Zimmerman MI, et al. Structure–function correlates of fibrinogen binding by *Acinetobacter* adhesins critical in catheter-associated urinary tract infections. Proc Natl Acad Sci 2023;120: e2212694120. https://doi.org/10.1073/pnas.2212694120.
[46] Kyriakidis I, Vasileiou E, Pana ZD, Tragiannidis A. *Acinetobacter baumannii* antibiotic resistance mechanisms. Pathogens 2021;10:373. https://doi.org/10.3390/pathogens10030373.
[47] Petersen K, Riddle MS, Danko JR, Blazes DL, Hayden R, Tasker SA, et al. Trauma-related infections in battlefield casualties from Iraq. Ann Surg 2007;245:803. https://doi.org/10.1097/01.sla.0000251707.32332.c1.
[48] Dallo SF, Weitao T. Insights into *Acinetobacter* war-wound infections, biofilms, and control. Adv Skin Wound Care 2010;23:169. https://doi.org/10.1097/01.ASW.0000363527.08501.a3.
[49] Gontijo AVL, Pereira SL, de Lacerda Bonfante H. Can drug repurposing be effective against carbapenem-resistant *Acinetobacter baumannii*? Curr Microbiol 2021;79:13. https://doi.org/10.1007/s00284-021-02693-5.
[50] Aguilar-Vega L, López-Jácome LE, Franco B, Muñoz-Carranza S, Vargas-Maya N, Franco-Cendejas R, et al. Antibacterial properties of phenothiazine derivatives against multidrug-resistant *Acinetobacter baumannii* strains. J Appl Microbiol 2021; 131:2235–43. https://doi.org/10.1111/jam.15109.
[51] Cruz-Muñiz MY, López-Jacome LE, Hernández-Durán M, Franco-Cendejas R, Licona-Limón P, Ramos-Balderas JL, et al. Repurposing the anticancer drug mitomycin C for the treatment of persistent *Acinetobacter baumannii* infections. Int J Antimicrob Agents 2017;49:88–92. https://doi.org/10.1016/j.ijantimicag.2016.08.022.
[52] Cheng Y-S, Sun W, Xu M, Shen M, Khraiwesh M, Sciotti RJ, et al. Repurposing screen identifies unconventional drugs with activity against multidrug resistant *Acinetobacter baumannii*. Front Cell Infect Microbiol 2019;8. https://doi.org/10.3389/fcimb.2018.00438.
[53] Eze EC, Chenia HY, Zowalaty MEE. *Acinetobacter baumannii* biofilms: effects of physicochemical factors, virulence, antibiotic resistance determinants, gene regulation, and future antimicrobial treatments. Infect Drug Resist 2018;11: 2277–99. https://doi.org/10.2147/IDR.S169894.
[54] Otsu N. A threshold selection method from gray-level histograms. IEEE Trans Syst Man Cybern 1979;9:62–6. https://doi.org/10.1109/TSMC.1979.4310076.